Available online at www.sciencedirect.com
ScienceDirect
Deep-Sea Research I 53 (2006) 1925–1940
DEEP-SEA RESEARCH PART I
www.elsevier.com/locate/dsri

Local remineralization patterns in the mesopelagic zone of the Eastern North Atlantic, off the NW Iberian Peninsula

C.G. Castro*, M. Nieto-Cid, X.A. Álvarez-Salgado, F.F. Pérez

CSIC, Instituto de Investigacións Mariñas, Eduardo Cabello 6, 36208 Vigo, Spain

Received 15 July 2005; received in revised form 29 August 2006; accepted 5 September 2006
Available online 27 October 2006

Abstract

The short-time-scale variability of the remineralization patterns in the domain of Eastern North Atlantic Central Waters (ENACW) off the NW Iberian Peninsula is studied based on biogeochemical data (oxygen, nutrient salts, total alkalinity, pH, dissolved organic matter and fluorescence of dissolved humic substances) collected weekly between May 2001 and April 2002. The temporal variability of inorganic variables points to an intensification of remineralization during the summer and autumn, with an increase of nutrients, total inorganic carbon and fluorescence and a decrease of oxygen. During the subsequent winter mixing, there is a biogeochemical reset of the system, with lower nutrients, total inorganic carbon and fluorescence and higher oxygen. In contrast to inorganic variables, the levels of dissolved organic matter in the ENACW seem to respond to short-term events probably associated with fast sinking particles, where solubilisation of organic matter prevails over remineralization. Applying a previously published stoichiometric model, we observed a vertical fractionation of organic-matter remineralization. Although there is a preferential remineralization of proteins and P compounds in the entire domain of ENACW, the percentage was higher in the upper ENACW ($\sigma < 27.10\,kg/m^3$) than in the lower; the percentage of N and P compounds in the oxidised organic matter was >80% for the upper ENACW and 63% for the lower. Likewise, the redissolution of calcareous structures contributes about 6% and 13% to the carbon regenerated in the upper and lower layers of ENACW, respectively.

Keywords: Water masses; Remineralization; Nutrients; Dissolved organic matter; Mesopelagic zone; Northeast Atlantic Ocean; European ocean margin

1. Introduction

The mesopelagic or the "twilight" zone, located between the base of the euphotic zone and 1000 m, plays important roles in ocean remineralization/respiration processes. Among these roles are its contribution to the metabolic state of the ocean, defined as the balance between in-situ primary production and total respiration (Smith and Hollibaugh, 1993), and its impact on the global carbon cycle (del Giorgio and Duarte, 2002; Arístegui et al., 2003; Karl et al., 2003; Hansell et al., 2004). del Giorgio and Duarte (2002) estimated a total respiration in the mesopelagic layer of ~24.5 Gt-C/yr, which represents around 37% of the total respiration of the open ocean (see their Table 1). However, they also state that there is an extremely large uncertainty (minimum 35%) in this estimate as

*Corresponding author. Tel.: +34 986 231930; fax: 34 986 292762.
E-mail address: cgcastro@iim.csic.es (C.G. Castro).

0967-0637/$ - see front matter © 2006 Elsevier Ltd. All rights reserved.
doi:10.1016/j.dsr.2006.09.002

respiration measurements below the euphotic zone are rarely done because of the lack of sufficiently sensitive techniques. Because of this lack and the importance of remineralization in the mesopelagic layer, the emerging global programs such as Integrated Marine Biogeochemistry and Ecosystem Research (IMBER) and Ocean Carbon Transport, Exchanges and Transformations (OCTET), are going to dedicate part of future efforts to the development of new methodologies.

The mesopelagic layer has been considered as the largest "heterotrophic digester" of the oceans (Benner, 2000). The nature and extension of the transformation and remineralization of organic matter through the mesopelagic layer affects the quantity and stoichiometry of material delivered to the deep sea and seafloor. The mesopelagic layer is also critical for the input of nutrients into the euphotic zone and subsequent control of primary production.

Zones especially important to mesopelagic biogeochemical processes are the regions of formation of modal waters, where thermocline subsurface waters are transferred yearly into the euphotic. Nutrient and dissolved organic matter (DOM) concentrations of the newly-formed modal waters depend on the concentrations of the subsurface thermocline waters just before the winter mixing and consequently on the remineralization that has occurred in the mesopelagic layer. This is the case for the Eastern North Atlantic Central Waters (ENACW), the main subsurface modal waters in the ventilated thermocline of the Eastern North Atlantic.

From observations of the thermohaline properties, Fiúza (1984) discerned two types of ENACW: those with temperatures $<13\,^{\circ}C$ (ENACW of subpolar origin; $ENACW_{SP}$) and those with temperatures $>13\,^{\circ}C$ (ENACW of subtropical origin; $ENACW_{ST}$). $ENACW_{SP}$ is formed north of ~43°N with winter-mixed layer depths between 400 and 600 m and, consequently, with high nutrient concentrations (nitrate concentrations between 3 and 10 μM at the time of formation; Castro, 1997; Pérez et al., 2005). Once formed, $ENACW_{SP}$ subducts and is conveyed southward as part of the anticyclonic circulation of the subtropical gyre (McCartney and Talley, 1982). $ENACW_{ST}$ is formed south of 43°N in shallower winter mixed layers (~200 m deep) and with lower nutrient levels (nitrate concentrations between 0.5 and 2 μM) and it is transported northward by the Portugal Coastal Undercurrent (PCUC) during the upwelling season and by the Portugal Coastal Counter Current (PCCC) during the rest of the year (Álvarez-Salgado et al., 1993; Castro et al., 1997).

Previous studies have been focused on remineralization in ENACW over the shelf (Álvarez-Salgado et al., 1993, 1997). From these studies, we know that ENACW gains mineralised nutrient as the upwelling season progresses and that nutrient enrichment is more intensified off the Galician west coast, off the Rías Baixas (Fig. 1), than on the northern coast. This intensification is caused by a longer residence time of the upwelled water and a higher input of particulate organic matter supplied by the Rías Baixas. In fact, this stronger nutrient enrichment due to remineralization on the west shelf is able to reduce the difference that would otherwise occur in nutrient concentrations between $ENACW_{SP}$, which usually upwells on the north coast, and $ENACW_{ST}$, upwelling on the west coast; thus the potential primary production controlled by upwelled nutrient levels is similar for the two regions. In the oceanic domain, Pérez et al. (1993) studied the remineralization patterns of the water masses at this eastern boundary with data collected on a series of hydrographic cruises carried out between 1982 and 1993. They studied mainly the spatial remineralization patterns and their relationship with the mixing and displacement of water masses in the region.

The aim of this paper is to have a first view of the temporal variability of the remineralization patterns in the mesopelagic layer of the northeast Atlantic, based on the chemical data collected with a weekly frequency at a station off the NW Iberian Peninsula between May 2001 and April 2002. Our interest arises because ENACW are the main source of

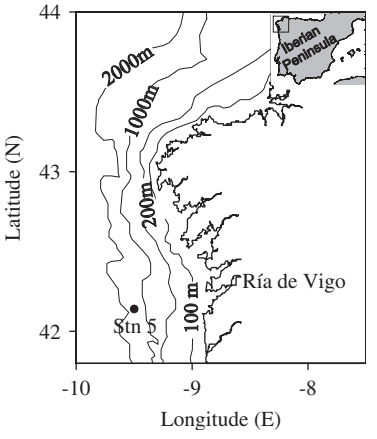

Fig. 1. Map of the study area, shelf-break waters of the NW Iberian upwelling system. The position of the sampling station is indicated. The isobaths of −100, −200, −1000 and −2000 m are depicted.

nutrients to the NW Iberian upwelling system; the sole upwelling region of Europe.

2. Material and methods

Stations on a transect from the coast to 85 km off the NW Iberian coast (Fig. 1) were sampled weekly between May 2001 and April 2002 in the framework of the DYBAGA (Dinámica Y Biogeoquímica annual en la plataforma GAllega: variación de corta escala) project. The aim of this project was to study on this short time scale the oceanographic conditions off the NW Iberian Peninsula. The basis for this paper is the hydrographic data collected at the most offshore station (Stn. 5), which corresponds to the oceanic reference for analysing the processes and hydrographic conditions over the shelf and inside the Ría de Vigo (see Nieto-Cid et al., 2004, 2005; Álvarez-Salgado et al., 2006).

The cruises were carried out on board R/V *Mytilus*. A total of 47 surveys were conducted, but unfortunately, because of bad weather we were not able to sample Station-5 on two occasions (November 7th, 2001, and April 2nd, 2002). Conductivity, temperature and pressure were measured with a SBE 911 CTD probe incorporated into a rosette sampler with 10-L PVC Niskin bottles. Salinity was calculated from conductivity measurements and the equation of UNESCO (1985). Samples for the analysis of dissolved oxygen, total alkalinity, pH, nutrient salts, dissolved organic carbon and nitrogen and fluorescence of dissolved humic substances were collected at 15 different depths in the water column from surface to the upper core of Mediterranean Water, with a more intense sampling at ENACW depths.

Dissolved oxygen was determined by Winkler potentiometric titration. The estimated analytical error was ± 1 μmol/kg. Total alkalinity was determined by potentiometric titration with HCl to a final pH of 4.4 (Pérez and Fraga, 1987). The analytical error was ± 2 μmol/kg. pH was analysed spectrophotometrically following Clayton and Byrne (1993). Total inorganic carbon (C_T) was estimated from pH and total alkalinity and the carbonic acid system equations with the carbonic acid and boric acid dissociation constants of Lueker et al. (2000). Nutrient samples were determined by segmented flow analysis with Alpkem autoanalyzers following Hansen and Grasshoff (1983) with some improvements (Mouriño and Fraga, 1985). The analytical errors were ± 0.02 μM for nitrite, ± 0.05 μM for nitrate, ammonium and silicate and ± 0.01 μM for phosphate. Dissolved organic carbon (DOC) and nitrogen (DON) were measured simultaneously with a nitrogen-specific Antek 7020 nitric oxide chemiluminescence detector, coupled in series with the carbon-specific infra-red gas analyser of a Shimadzu TOC-5000 organic carbon analyser (Álvarez-Salgado and Miller, 1998). The analytical errors were ± 1 μM for DOC and ± 0.2 μM for DON.

The fluorescence of dissolved humic substances (FDOM) was measured with a Perkin Elmer LS 55 luminescence spectrometer working with a xenon discharge lamp, equivalent to 20 kW for 8 μs duration, and a 1-cm quartz fluorescence cell. Milli-Q water was used as a reference for fluorescence analysis, and the intensity of the Raman peak was checked several times every working day. Discrete FDOM analyses were executed within a few hours after sample collection at Ex/Em wavelength 320/410 nm. Four replicates were performed. A four-point standard curve was prepared daily with a mixed standard of quinine sulphate (QS) in sulphuric acid 0.05 M. The equivalent concentration of every peak was determined by subtracting the average peak height from the blank height, and dividing by the slope of the standard curve. Fluorescence units were expressed in ppb equivalents of QS (ppb QS) with an analytical error of ± 0.1 ppb QS; for more details see Nieto-Cid et al. (2005).

3. Stoichiometric model

3.1. Separation of physical and biogeochemical components of the distribution of chemical parameters

The ENACW off the NW Iberian Peninsula occupies the water column in the permanent thermocline, from the salinity minimum at ~450–500 m deep, characteristic of the fresher and colder portions of $ENACW_{SP,}$ to a salinity maximum just below the seasonal thermocline (~50–100 m depth), characteristic of the saltier and warmer portions of $ENACW_{ST}$. This upper limit could be even shallower during the autumn and winter period.

On a TS diagram, the cluster of points corresponding to ENACW is better defined by two straight lines, i.e. three end members taking into account the subtropical and subpolar branches of ENACW (Fig. 2; Castro et al., 1998). A three-end-member mixing problem can be solved by a linear regression analysis involving two conservative variables, salinity and temperature. An anomaly (ΔY)

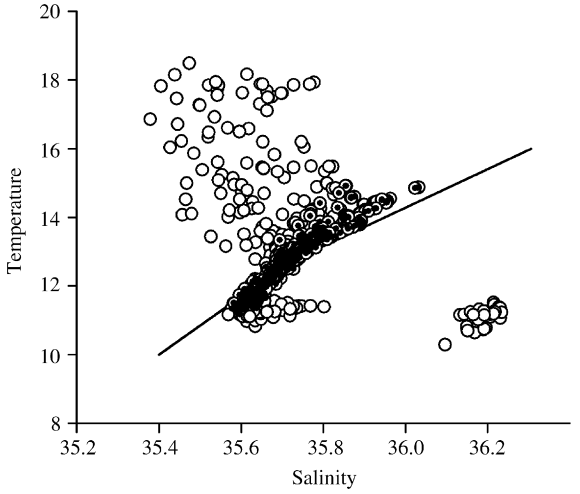

Fig. 2. Temperature (°C)—salinity diagram for all the water samples collected during the DYBAGA project at Station-5 from May 2001 to April 2002. Black dotted points correspond to ENACW samples. Solid line is the reference line for ENACW, defined by Fiúza (1984).

can be defined for each chemical parameter (Y)

$$\Delta Y = Y - a_0 - a_1 \times S - a_2 \times T, \tag{1}$$

where a_0, a_1 and a_2 are the coefficients of the linear multiple regression of Y with salinity and temperature. ΔY retains only the variability associated with the remineralization that occurs in waters with AOU > 0, i.e. the decomposition of organic matter and the dissolution of calcareous and siliceous structures.

It is important to remark that our station is located in the ventilation region of ENACW. Consequently, some vintages of ENACW acquires their thermohaline and chemical properties in contact with the atmosphere by the formation of winter mixed layers of about 200–300 m deep at the study latitude. We have also included these data in our analysis as we are interested in the comparison of the different biogeochemical properties of ENACW on a seasonal scale. We have included only those samples with AOU > 0, based on the assumption that the water mass is formed in equilibrium with the atmosphere and subsequently subducted (Pérez et al., 2005).

3.2. Regression analysis of nutrient anomalies

The best fit between any couple of nutrient anomalies (ΔX, ΔY) was obtained by minimising the function

$$\sum_i \left[\left(\Delta X_i - \Delta \hat{X}_i\right)^{w_X} \times \left(\Delta Y_i - \Delta \hat{Y}_i\right)^{w_Y} \right]^2, \tag{2}$$

where $\Delta \hat{X}_i$ and $\Delta \hat{Y}_i$ are the expected values of ΔX and ΔY from the linear regression equation, i.e. $\Delta \hat{Y}_i = m \times \Delta X_i$ and $\Delta \hat{X}_i = \Delta Y_i / m$, with m being the slope of the correlation between ΔX and ΔY; w_X and w_Y are weights for variables X and Y, with w_X, $w_Y \geqslant 0$ and $w_X + w_Y = 1$. The weight factors were estimated as a function of the precision of the analytical determination of the variable (er) compared with the standard deviation of the set of measurements of that variable for water samples with AOU > 0 (SD). For a given couple of variables X and Y

$$w_X = \left(\frac{\mathrm{er}_X}{\mathrm{SD}_X}\right) \Big/ \left(\frac{\mathrm{er}_X}{\mathrm{SD}_X} + \frac{\mathrm{er}_Y}{\mathrm{SD}_Y}\right). \tag{3}$$

Minimising Eq. (2) considering the weight factor of Eq. (3) ensures that the slopes of the linear regression equations account for the relative precision (er/SD) of the pairs of nutrient anomalies that are correlated each time. Combining and rearranging Eqs. (2) and (3), it results that the function to minimise is

$$\sum_i \left[\left(\Delta X_i - \frac{\Delta Y_i}{m} \right)^{w_X} (\Delta Y_i - m \Delta X_i)^{w_Y} \right]^2 = \left(\frac{1}{m}\right)^{2w_X} \sum_i (\Delta Y_i - m \Delta X_i)^2. \tag{4}$$

In addition, the value of the slope (m) that makes Eq. (4) minimum is

$$m = \frac{1 - 2w_X}{2 - 2w_X} \frac{\sum_i \Delta X_i \Delta Y_i}{\sum_i \Delta X_i^2} + \frac{\sqrt{\left((1 - 2w_X) \sum_i \Delta X_i \Delta Y_i \right)^2 + 4 w_X (1 - w_X) \sum_i \Delta X_i^2 \sum_i \Delta Y_i^2}}{2(1 - w_X) \sum_i \Delta X_i^2}. \tag{5}$$

Table 1
Ratio of the analytical error of the chemical variables (er) and the standard deviation of their anomalies (SD) for ENACW samples from the NW Iberian shelf break. Dimensionless

Variable	er/SD		
	Upper	Middle	Lower
	($\sigma_0 < 26.95$)	($26.95 < \sigma_0 < 27.10$)	($\sigma_0 > 27.10$)
ΔO_2	0.04	0.08	0.11
ΔC_{TC}	0.21	0.38	0.21
ΔNO_3	0.06	0.11	0.18
ΔP	0.21	0.37	0.52
ΔSi	0.08	0.16	0.18
ΔCa	4.10	3.86	3.79
ΔDOC	0.34	0.33	0.35
ΔDON	0.33	0.28	0.29
$\Delta FDOM$	0.83	1.43	2.25

Therefore, m is an intermediate case between: (1) the slope of a Type I regression (which should be applied when $w_X = 0$, $w_Y = 1$), $m = \sum_i(\Delta X_i \times \Delta Y_i)/\sum_i \Delta X_i^2$ and (2) the slope of a Type II regression (which should be applied when $w_X = w_Y = 0.5$), $m = \sqrt{\sum_i \Delta Y_i^2 / \sum_i \Delta X_i^2}$ (Sokal and Rohlf, 1995). Table 1 summarizes the values of er/SD for all the study variables at the different isopycnal layers.

3.3. Conversion of nutrient anomalies into the chemical composition of biogenic materials

From the nutrient anomaly ratios, we obtain an average elemental composition of the material being remineralized in the water column. Subsequently, we estimate the percentage of the main groups of biomolecules composing marine plankton following the method described by Fraga (2001). This author reviewed in detail the average elemental composition within each major group: proteins (Prt), carbohydrates (Cho), lipids (Lip), phosphorus compounds (Pho) and pigments (Chl). Table 2 summarizes the average chemical formulas of these groups of biomolecules. Considering the chemical formulas in Table 2, the proportions of the different biomolecules can be calculated from the O_2, C_T, NO_3^- and HPO_4^{2-} anomalies. The levels of NO_2^- and NH_4^+ in ENACW are relatively low, <0.1 and $<0.2\,\mu M$, respectively. Equations describing the remineralization of proteins, carbohydrates, lipids and phosphorus compounds can be written as

Table 2
Chemical composition of the main organic products of synthesis and early degradation of marine phytoplankton according to Fraga (2001)

	Chemical formula
Proteins	$C_{138}H_{217}O_{45}N_{39}S$
Carbohydrates	$C_6H_{10}O_5$
Lipids	$C_{53}H_{89}O_6$
Phosphorus compounds	$C_{45}H_{76}O_{31}N_{12}P_5$
Pigments	$C_{46}H_{52}O_5N_4Mg$
Average composition	$C_{106}H_{171}O_{41}N_{16}P$

$$C_{138}H_{217}O_{45}N_{39}S + 144O_2 + 103OH^- \rightarrow 138HCO_3^- + 39NO_3^- + SO_4^{2-} + 15H_2O, \quad (6)$$

$$C_6H_{10}O_5 + 6O_2 + 6OH^- \rightarrow 6HCO_3^- + 5H_2O, \quad (7)$$

$$C_{53}H_{89}O_6 + 72.25O_2 + 53OH^- \rightarrow 53HCO_3^- + 44.5H_2O, \quad (8)$$

$$C_{45}H_{76}O_{31}N_{12}P_5 + 47.75O_2 + 45OH^- \rightarrow 45HCO_3^- + 12NO_3^- + 5HPO_4^{2-} + 13.5H_2O. \quad (9)$$

And the corresponding linear system of mass balance equations is

$$\Delta O_2 = 144 \times \Delta Prt + 6 \times \Delta Cho + 72.25 \times \Delta Lip + 47.75 \times \Delta Pho, \quad (10)$$

$$\Delta C_T = -138 \times \Delta Prt - 6 \times \Delta Cho - 53 \times \Delta Lip - 45 \times \Delta Pho, \quad (11)$$

$$\Delta NO_3 = -39 \times \Delta Prt - 12 \times \Delta Pho, \quad (12)$$

$$\Delta P = -5 \times \Delta Pho. \quad (13)$$

Inorganic carbon is produced during the degradation of organic matter and calcareous ($CaCO_3$) structures. Since Eqs (6)–(9) refer only to the oxidation of organic carbon, the correction for the precipitation/dissolution of $CaCO_3$ must be determined from C_T variability (C_{TC})

$$C_{TC} = C_T - \tfrac{1}{2} \times TA_P, \quad (14)$$

where TA_P is the potential alkalinity, calculated following Broecker and Peng (1982):

$$TA_P = TA + \lfloor NO_3^- \rfloor. \quad (15)$$

4. Results and discussion

4.1. Temporal variability

During the study period, we captured the most characteristic dynamic scenarios of the NW Iberian upwelling system (Fig. 3). From the beginning of the study period until September 22nd, water-column structure was characterized by thermal stratification in the upper 100 m in spite of the prevailing upwelling-favourable northerly winds. After September 22nd, there was a wind reversal, but water-

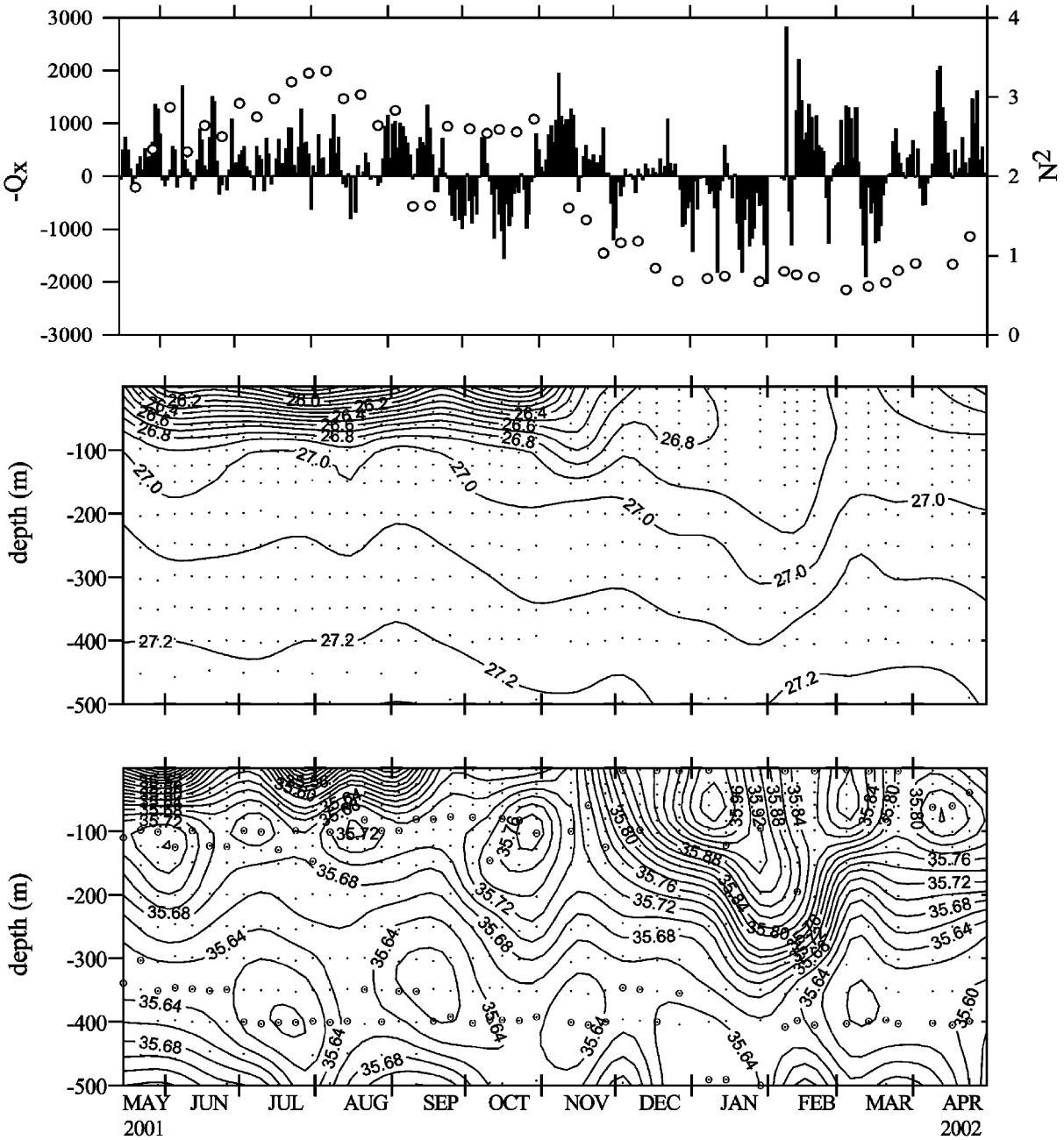

Fig. 3. Time series of the offshore Ekman transport (-Qx) calculated with wind data provided by the SeaWatch Buoy Meteorological Observatory (http://www.puertos.es) and Brünt-Väiäsala frequency (N^2; open circles) (a); density anomaly (b) and salinity (c) from May 2001 to April 2002. The open circles on plot (b) correspond to the upper and lower limit of ENACW. Offshore Ekman transport in $m^3/(s\,km)$, N^2 in s^{-2} and density anomaly in kg/m^3.

column stratification was still high because of intense continental runoff from the adjacent Rías Baixas. After that, there was a sharp decrease of stratification, and after November 29th, prevailing southerly winds favoured the presence of high salinity waters (salinity ~35.90). The period from the beginning of February until mid-March corresponded to the winter mixing, with salinity values slightly fresher than during the previous periods. Winter mixed-layer depths varied between 100 and 200 m, with maximum deepening at the beginning of February 2002.

The ENACW occupied depths between 100 and 400 m (delimited by white circles on the salinity time series; Fig. 3c), being even shallower during the autumn and winter seasons. We observed ENACW of subpolar and subtropical origins, as shown on the TS diagram for all the bottle samples collected at station 5 (Fig. 2). Here, ENACW is clearly recognised by the cluster of points with an almost linear TS relationship varying between a salinity minimum of 35.58 (T~11.34 °C) and a maximum of 36.02 (T~14.85 °C). These thermohaline characteristics are very similar to those previously described by Fiúza (1984) for this water mass.

Our data also support the seasonal cycle of stratification/homogenisation in the Portugal Coastal Counter Current (PCCC) established by Álvarez-Salgado et al. (2003) based on only seven cruises off the Galician Coast. The time variability of the salinity maximum for the ENACW upper limit tracks the evolution of the PCCC core. During the upwelling season (May 15th–September 22nd), a well defined subsurface salinity maximum was maintained beneath the seasonal thermocline. This salinity maximum clearly defines the core of the poleward current conveying $ENACW_{ST}$. The core was characterized by nitrate levels between 4 and 8 μM, DON between 4 and 5 μM, and ~2.5 ppb QS (2.3–2.7) (Figs. 3 and 4). After the transitional period to low stratification (October 30th–November 29th), the ENACW upper limit surfaced, and we observed $ENACW_{ST}$ saltier than 35.94. These $ENACW_{ST}$ volumes were also characterized by low nitrate concentrations (<3 μM), relatively high DOM concentrations (DON >4.5 μM and DOC >62 μM; distribution not shown) and ~2.0 ppb QS (1.5–2.5). During the subsequent winter mixing, the salinity maximum of the ENACW upper limit decreased (~0.06), though it still remained high. The recently formed $ENACW_{ST}$ was enriched in inorganic nutrients and FDOM and had relatively low DOM concentrations (Figs. 4b and d). The salinity minimum corresponding to the ENACW lower limit was about the isopycnal level of 27.17 kg/m^3 (~350–400 m), except during the winter mixing period, when the ENACW lower limit deepened to ~500 m.

4.2. Seasonal pattern of remineralization

The high-frequency sampling of the DYBAGA project allowed us to study the temporal variability of nutrient enrichment due to remineralization in the ENACW domain. The time series of oxygen, nitrate, DON and FDOM followed a similar trend and strongly correlated with temperature ($r>0.70$; $p<0.001$ for the four cases) because of mixing of different ENACW vintages. The residual variability not explained by thermohaline properties corresponds to the aging that ENACW experienced due to biogeochemical or ventilation processes, as we discuss below. Fig. 5 shows the oxygen, nitrate, DON and FDOM anomalies of ENACW waters for the study year. Positive nutrient anomaly (negative oxygen anomaly) is associated with higher than average nutrient concentration for this water parcel due to remineralization of organic matter. Negative nutrient anomaly corresponds with lower-than-average nutrient concentration, and it can be associated with ventilation.

The temporal distributions of oxygen and nitrate anomalies (Figs. 5a and b) are very similar ($r=-0.90$; $p<0.001$) and suggest a seasonal pattern modulated by remineralization/ventilation processes in the ENACW domain. As the upwelling season progressed, we observed an aging of the subsurface waters. Thus oxygen anomalies decreased (nitrate anomalies increased) between May 15th and September 18th, 2001, reflecting the decomposition of organic matter formed during the productive spring and summer seasons. However, the most negative oxygen anomalies (highest nitrate enrichment) were recorded during the autumn (September 25th and November 27th, 2001), associated with $ENACW_{ST}$ conveyed northward in the PCUC/PCCC. The situation dramatically changed during the winter, when maximum ventilation occurred and the recently formed ENACW was characterized by high oxygen and low nitrate levels compared with the average. The lowest oxygen anomalies were observed at the sea surface, in contrast with the vertical structure of the anomalies during the previous periods, when the

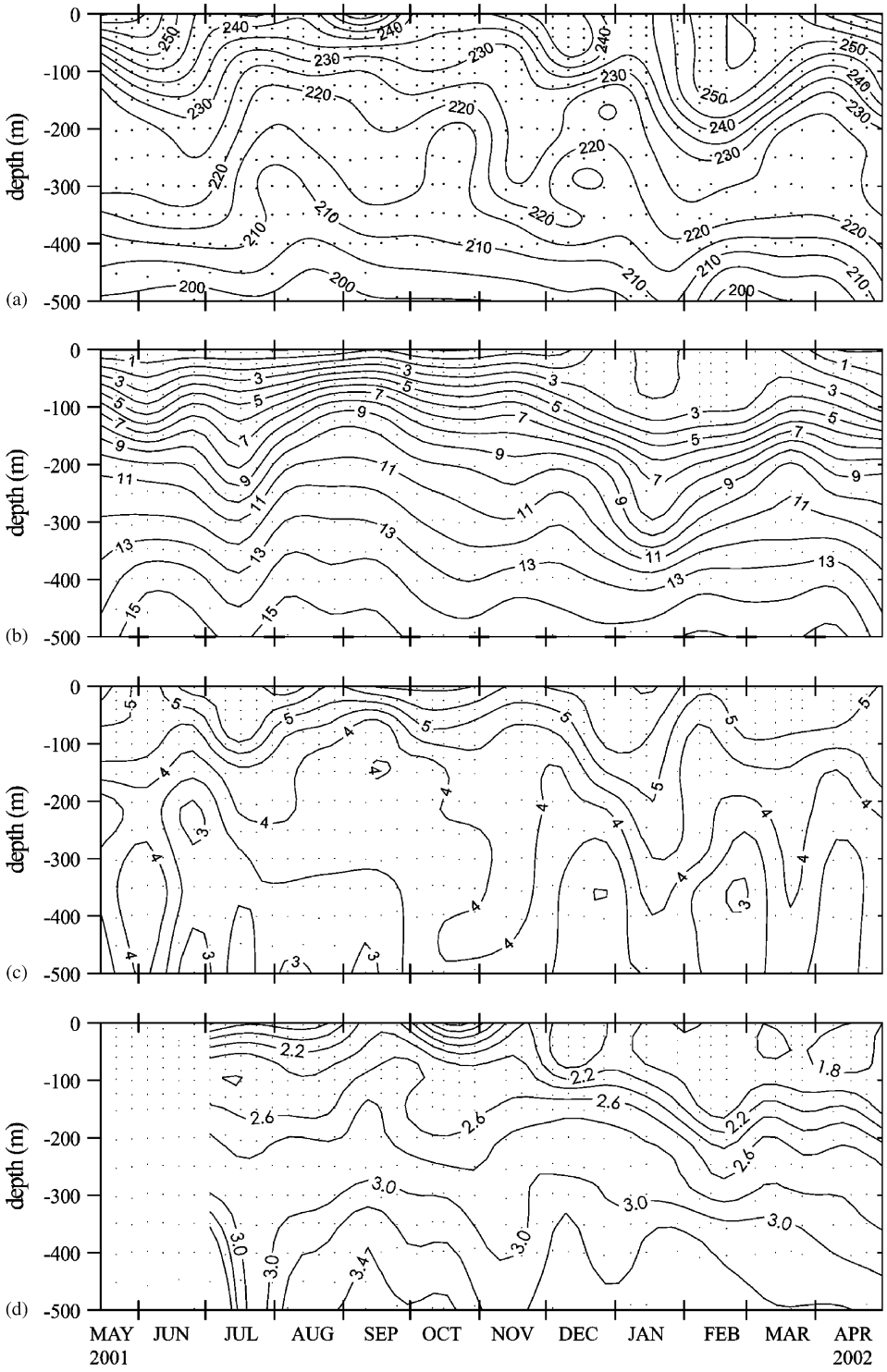

Fig. 4. Time series of oxygen (a), nitrate (b), dissolved organic nitrogen (c) and fluorescence of dissolved humic substances (d) for the study period. Oxygen, nitrate and DON in μM and FDOM in ppb QS.

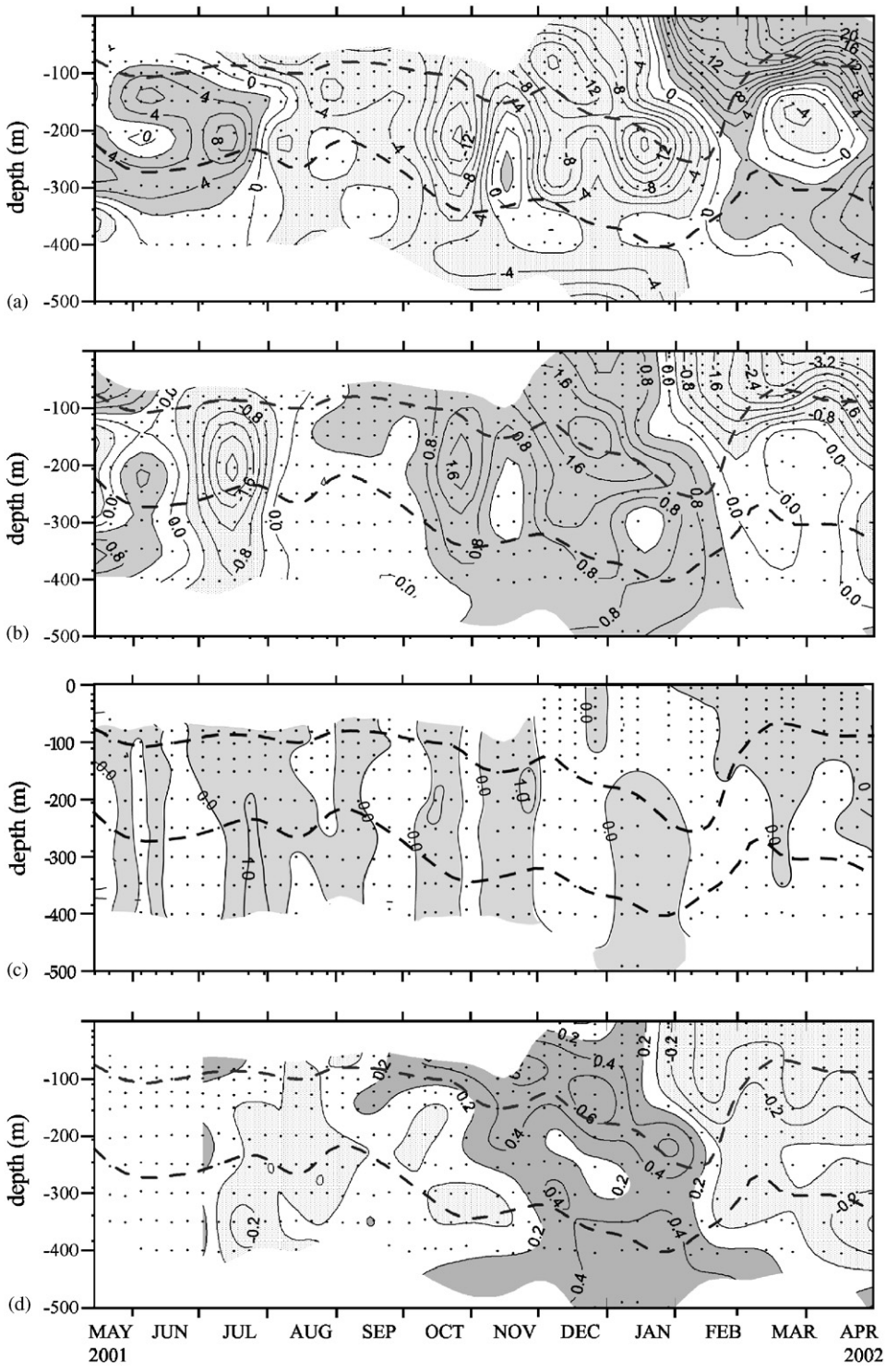

Fig. 5. Time series of the anomalies for oxygen (a), nitrate (b), dissolved organic nitrogen (c) and fluorescence of dissolved humic substances (FDOM) (d) during the study period. Oxygen, nitrate and DON in μM and FDOM in ppb QS.

extreme anomalies were located at the base of the nutricline. This pattern was still observed during the subsequent spring bloom.

The temporal distribution of DON anomalies (Fig. 5c) does not follow such a clear seasonal pattern. The only striking feature was the high positive DON anomalies observed at the beginning of the winter mixing period and the positive values for the subsequent spring period. Before that, the DON-anomaly time series seems to respond to short-term events of DON enrichment in the entire water column; i.e., there is a homogenised distribution of DON anomaly over the entire water column.

Finally, the temporal distribution of FDOM anomalies (Fig. 5d) shows the same pattern as oxygen and nitrate. Fluorescence anomalies increased with the progression of the upwelling season until September. Maximum anomalies were also reached in winter, following the 26.95 kg/m^3 isopycnal at the base of the pycnocline, where metabolic processes were high. The lowest anomalies were observed at the sea surface at the end of winter and beginning of spring, coinciding with high oxygen and low nitrate anomalies.

4.3. Fractionation of remineralization in the domain of central waters

One further point to study is the fractionation of organic matter remineralization in the water column. Fractionation has important consequences on the global carbon cycle. The amount and depth at which dissolved inorganic carbon is released by remineralization determines the strength of the biological pump for drawdown of atmospheric CO_2 (Shaffer et al., 1999).

With this in mind, we have "vertically" divided the ENACW domain into three isopycnal ranges, and we now examine the remineralization ratios obtained from the correlations of the anomalies of the chemical variables for each density interval. The upper level extends from the shallow salinity maximum to the 26.95 kg/m^3 isopycnal, the density horizon of maximum nutrient and oxygen anomaly, corresponding to $ENACW_{ST}$. The lower level extends from the 27.10 kg/m^3 isopycnal to the deep salinity minimum and corresponds to $ENACW_{SP}$. Waters at intermediate density values constitute the middle layer.

In Table 3, we present the results. The low $\Delta O_2/\Delta P$ and $\Delta O_2/\Delta NO_3$ ratios relative to the classical Redfield ratios suggest a preferential remineralization of protein-rich organic matter. For the same region, Álvarez-Salgado et al. (2003) obtained $\Delta O_2/\Delta C_{TC}/\Delta N/\Delta P$ remineralization ratios of $113\pm3/108\pm12/16.7\pm0.6/1$ for ENACW between the 26.60 and 27.20 kg/m^3 isopycnals based on a series of seven cruises carried out between 1983 and 1998. Similar to our results, these molar ratios point to a preferential remineralization of protein-rich organic matter.

The biochemical composition of the mineralised organic matter can be obtained from these $O_2/C/N/P$ molar ratios by solving the determined system of linear Eqs. (10)–(13), and it is summarised in Table 4. It should be noted that the $\Delta O_2/\Delta C_{TC}$ ratio cannot be directly used because it is affected by the differential dissolution of anthropogenic CO_2

Table 3
Regression coefficient (r), slope and standard error of the slope of the correlation between selected pairs of nutrient anomalies for samples of the upper, middle and lower levels of ENACW off NW Spain

	Upper			Middle			Lower		
	($\sigma_0<26.95$)			($26.95<\sigma_0<27.10$)			($\sigma_0>27.10$)		
	r	Slope	Error	r	Slope	Error	r	Slope	Error
$\Delta O_2/\Delta C_{CT}$	−0.957	−1.22	0.04	−0.877	1.34	0.06	−0.750	−1.4	0.2
$\Delta O_2/\Delta NO_3$	−0.958	−6.9	0.2	−0.780	−6.7	0.4	−0.597	−8.9	1.2
$\Delta O_2/\Delta P$	−0.933	−125	5	−0.805	−139	8	−0.650	−154	18
$\Delta DOC/\Delta DON$	0.250	6	3	0.465	5	1	0.468	5	2
$\Delta DON/\Delta NO_3$	−0.430	−0.17	0.04	−0.228	ns	ns	0.114	ns	ns
$\Delta Ca/\Delta Corg$	0.708	0.07	0.01	0.226	0.07	0.02	0.353	0.14	0.04
$\Delta Si/\Delta Ca$	0.697	1.2	0.1	0.166	1.1	0.5	0.213	1.1	0.5
$\Delta NO_3/\Delta Si$	0.868	2.8	0.1	0.707	3.1	0.2	0.429	2.2	0.5
$\Delta FDOM/\Delta NO_3$	0.885	0.18	0.01	0.616	0.13	0.02	0.385	0.11	0.05

Table 4
Average chemical composition (phosphorus compounds, proteins, and carbohydrates) of the products of early degradation of marine phytoplankton photosynthesis as obtained from inorganic nutrients in %(w/w)

	Upper	Middle	Lower	Redfield
	($\sigma_0 < 26.95$)	($26.95 < \sigma_0 < 27.10$)	($\sigma_0 > 27.10$)	
P compounds	14.7 ± 0.7	13.4 ± 0.4	12 ± 2	12.0
Proteins	67 ± 3	72 ± 2	51 ± 8	47.1
Carbohydrates	11 ± 8	8 ± 5	22 ± 25	24.4
Lipids	8 ± 4	7 ± 2	15 ± 14	16.5
Formula	$C_{84}H_{133}O_{32}N_{18}P$	$C_{92}H_{146}O_{34}N_{21}P$	$C_{109}H_{175}O_{44}N_{17}P$	$C_{106}H_{171}O_{41}N_{16}P$

throughout the seasonal cycle. Therefore, we tested the range of $\Delta O_2/\Delta C_{TC}$ values that produce at least 5% remineralization of phosphorus compounds, proteins, lipids and carbohydrates (Anderson, 1995). It ranges from 1.47 to 1.51 in the upper, 1.50 to 1.52 in the middle and 1.35 to 1.47 in the lower layer. The lower is the only layer where the expected and observed $\Delta O_2/\Delta C_{TC}$ values (1.4 ± 0.2) coincided, because it is less affected by the penetration of anthropogenic carbon.

In the upper and middle layers, the average biochemical composition of the remineralized organic matter is richer in N (Prt) and P (Pho) compounds (>80%) and poorer in carbon (Cho and Lip) compounds (<20%) than Redfield's mean (59% and 40%, respectively; see Table 4). On the other hand, the biochemical composition of the lower layer is comparable to Redfield's values: the contribution of Prt + Pho compounds decreases to 63%, whereas the percentage of Lip + Cho increases to 37%. In this sense, our results corroborate the study of Li and Peng (2002). They found a systematic decrease in protein content of remineralized organic matter from the North Atlantic to the North Pacific, following the conveyor-belt circulation (see their Table 3). Also Brea et al. (2004), analysing the nutrient remineralization ratios in the eastern South Atlantic, found that proteins were remineralized preferably over other compounds in the domain of South Atlantic Central Waters , while for deeper water masses there was a decrease in the protein proportion.

The comparison of the remineralization and biochemical composition for the three layers shows a preferential remineralization of protein and phosphorus compounds in the upper and middle layers and of carbohydrates and lipids in the lower layer, indicating a vertical fractionation in the domain of ENACW. Previous work (Castro et al., 1998; Thomas et al., 2002), also examining stoichiometric ratios from chemical data, indicates a vertical fractionation in the eastern North Atlantic between depths above and below the main thermocline. These authors found a higher release of nutrients over inorganic carbon in the upper layer. Likewise, Minster and Boulahdid (1987), revisiting the method of Takahashi et al. (1985), estimated the Redfield ratios along several isopycnals in the North Atlantic and found no fractionation of organic matter remineralization for the two shallower levels (27.00 and 27.20 kg/m^3 isopycnals); however, they found a decrease in the $\Delta O_2/\Delta P$ for deeper levels (27.40 and 27.80 kg/m^3 isopycnals).

There are few papers dealing with shallow remineralization processes, and all of them are focused on the oligotrophic Subtropical Gyres of the North Pacific and North Atlantic Oceans (Jenkins and Goldman, 1985; Sarmiento et al., 1990; Emerson and Hayward, 1995; Abell et al., 2000). For the North Pacific Subtropical Gyre, Emerson and Hayward (1995) described the presence of subsurface waters with negative preformed nitrate, which they suspect is due to the oxidation of DOM rich in carbon Subsequently, Abell et al. (2000) corroborated this hypothesis with DOM data and found different remineralization regimes for central waters that outcrop inside the gyre and those outcropping just north of it. Along isopycnals that outcrop inside the gyre, the C:N remineralization ratio is 30 ± 10, from the oxidation of an excess of labile DOC produced by nitrogen-fixing organisms, while for deeper isopycnals the C:N ratio is 8 ± 1. By comparison with this situation, we hypothesise different remineralization patterns for $ENACW_{ST}$ and $ENACW_{SP}$ taking into account their different oceanographic regime, the same as the above result.

Likewise, we do not observe an increasing ratio of $\Delta DOC:\Delta DON$ as we would expect considering a

preferential remineralization of nitrogen over carbon, as reported for other regions (Hopkinson et al., 1997; Hopkinson and Vallino, 2005; Loh and Bauer, 2000; Hung et al., 2003). In fact, the C:N molar ratio of the dissolved organic matter fraction is low for the three layers (Table 3) and similar to the classical Redfield ratio of 6.6, suggesting the remineralization of labile dissolved organic matter.

4.4. Remineralization of siliceous and calcareous structures

During the whole period, the calcite saturation profile varies from 3.5 times in subsurface waters to 2.5 at 500 m. Since the upper ocean is $CaCO_3$ supersaturated (Takahashi et al., 1981; Broecker and Peng, 1982), carbon regeneration at that level is predominantly due to the oxidation of organic carbon (Honjo et al., 1982; Honjo and Manganini, 1993). Milliman et al. (1999) proposed in a review of the global carbonate budget that 60–80% of the biogenic $CaCO_3$ dissolves in the upper 1000 m, above the lysocline, as a result of biological mediation in special microenvironments such as marine snow aggregates and invertebrate guts. The ratio between soft and hard biogenic material decomposition rates varies with depth in the oceans (Broecker and Peng, 1982). These authors, using the Geochemical Ocean Section Study (GEOSECS) data set, estimated a $\Delta Ca/\Delta Corg$ molar ratio of ~0.1 for the permanent thermocline and ~0.5 for deep waters. Recently, for the eastern North Atlantic Ocean, Pérez et al. (2002) fit to a polynomial depth function, the vertical profile of the $\Delta Ca/\Delta Corg$ ratio, which varies from 0.05 in the upper layer to 0.55 in deep waters. The vertical variation of $\Delta Ca/\Delta Corg$ ratio from 0.07 ± 0.01 in the upper level to 0.14 ± 0.04 in the lower level (Table 3) fits well with this vertical pattern.

Biogenic silica also dissolves in the deep ocean as sinking particles falling from the photic layer. Most of the silica dissolution takes place below the main thermocline. The high covariation between alkalinity and silicate profiles in open-ocean deep waters (Brewer et al., 1995; Broecker and Peng, 1982) is probably due to the biologically mediated dissolution of these hard structures in the microenvironments created by marine snow, zooplankton guts, etc. A mean $\Delta Si/\Delta Ca$ molar decomposition ratio of ~2 can be proposed according to the open ocean $CaCO_3$ and opal decomposition rates in the water column (Milliman et al., 1999; Treguer et al., 1995). According to Berger and Herguera (1992), a $\Delta Si/\Delta Ca$ ratio of 1.4 is expected for an area with a mean organic carbon flux of 10 mmol/m^2/d, which is in close agreement with the productivity of the eastern North Atlantic Ocean (Martin et al., 1993). Lower $\Delta Si/\Delta Ca$ ratios, around 1.05, were measured in sediment traps deployed at the North Atlantic Bloom Experiment (NABE) site below 3100 m (Newton et al., 1994). In this study, the $\Delta Si/\Delta Ca$ molar ratio was constant with depth at 1.1 (Table 3), which fits within the previous oceanic values and those found by Álvarez-Salgado et al. (2006) on the adjacent NW Iberian shelf. The $\Delta Si/\Delta Ca$ values of 2.5 ± 0.6 in the Ría de Vigo decreasing to 1.3 ± 0.2 on the shelf are consistent with the $\Delta Si/\Delta Ca$ value of 1.1 at the shelf break, following the expected seaward decrease of organic-matter flux.

Opal dissolution was high compared with organic-matter decomposition: the $\Delta NO_3/\Delta Si$ molar ratios show a vertical variability from 2.8 ± 0.1 in the upper layer to 2.2 ± 0.5 in the lower layer (Table 3). This vertical gradient suggests a relative increase of opal dissolution with depth in the ENACW, in agreement with an increase of the biogenic silica dissolution in deeper waters. On the other hand, these values are consistent with the seaward increase of $\Delta NO_3/\Delta Si$ from the inner NW Iberian shelf. Álvarez-Salgado et al. (2006) estimate $\Delta NO_3/\Delta Si$ molar ratios of 1.1 ± 0.1 in the Ría de Vigo and 1.8 ± 0.1 on the middle shelf. Assuming a theoretical $\Delta NO_3/\Delta Si$ ratio of ~1 for diatoms (Brzezinski, 1985), it results that diatoms represent from 90% in the Ría de Vigo to 35% in the upper layer at shelf break of the remineralized biogenic matter. The percentage increases to 45% in the lower ENACW layer.

4.5. Contribution of DOM to remineralization in the domain of central waters

Another important question is the contribution of DOM to the remineralization of organic matter in the domain of ENACW. We have estimated this contribution from the slope of ΔDON vs. ΔNO_3 and ΔDOC vs. ΔC_{TC} (Table 3). We have obtained a significant correlation between ΔDON and ΔNO_3 only at the shallower isopycnal level ($\sigma < 26.95$ kg/m^3) and no correlation for the other two levels. For ΔDOC vs. ΔC_{TC} we did not find any correlation for any of the three levels. On the other hand, we did observe a significant correlation (Table 3) between ΔDOC and ΔDON for the three levels, being even

more significant for the two deepest levels in spite of there being no correlation between ΔDON and ΔNO_3 and ΔDOC and ΔC_{TC}. From these results, we suggest that DON accounted for ~17% of organic matter remineralization at the shallower ENACW level ($\sigma < 26.95\,kg/m^3$). At this level, there is a preferential remineralization of nitrogen vs. carbon, as the lack of correlation between ΔDOC vs. ΔC_{TC} indicates. However, neither DON nor DOC contributes significantly to organic matter remineralization for the densest levels of ENACW, but still there are significant correlations between ΔDOC and ΔDON with low slopes (6 ± 3, 5 ± 1, 5 ± 2 for upper, middle and lower levels, respectively), pointing to relatively young (highly reactive; "labile" or "semi-labile") DOM (Hopkinson and Vallino, 2005). From the temporal distribution of DON anomalies (Fig. 5c), we suggest that the export of relatively reactive DOM is due to the leaking of DOM from sinking organic matter. That is, the observed plumes of DOM anomalies can be explained under the scenario described by Azam and Long (2001) where bacteria attracted to the sinking organic particles solubilise these particles, converting sinking organic matter into DOM in such a way that the rate of solubilisation is much higher than the rate of remineralization.

The contribution of DON to remineralization (~17%) for shallower ENACW ($\sigma < 26.95\,kg/m^3$) is lower than values obtained on the ría and shelf during the same study period (~20% and 30%, respectively; Álvarez-Salgado et al., 2006). On the continental shelf of Georges Bank, where upwelling of nutrient rich deep waters also occurs, Hopkinson et al. (1997) estimated that ~19% of remineralized N in the entire water column is derived from the export and decomposition of DOM. Abell et al. (2000) analysed the contribution of total organic carbon (TOC) and nitrogen (TON) to organic matter oxidation at different isopycnal levels for a meridional transect in the eastern subtropical North Pacific. They observed a situation completely different to that previously described for the NW Iberian upwelling system. They found that for isopycnals outcropping in the subtropical gyre, TOC and TON contribute 70% and 20%, respectively. In contrast, along isopycnals that outcrop to the north of the gyre, both TOC and TON contribute 30% to organic matter remineralization. They explained this preferential remineralization of TOC relative to TON by the excess of labile TOC produced during nitrogen fixation in the subtropical region.

4.6. The potential of the fluorescence of dissolved organic matter to trace remineralization processes in the central waters domain

The contribution of humic substances to the DOC pool was estimated using a conversion factor of $2.67\pm0.06\,\mu M$ C (ppb QS)$^{-1}$ obtained with a commercial fulvic acid (Nieto-Cid et al., 2005). On this basis, $9\pm2\%$ of DOC in the ENACW upper layer was humic substances, increasing to $12\pm1\%$ and $14\pm1\%$ in middle and lower layers, respectively. These numbers are in the range of those provided by Obernosterer and Herndl (2000) in the Adriatic Sea ($15\pm7\%$), but considerably lower than those proposed by the same authors in the North Sea ($43\pm7\%$), because of the higher terrestrial contributions in this last ecosystem.

Remineralization involves an increase in the concentration of nutrients and decrease in oxygen and organic matter concentrations. It was confirmed that these changes are accompanied by increase in FDOM (Chen and Bada, 1992; Hayase and Shinozuka, 1995; Wedborg et al., 1998; Nieto-Cid et al., 2005, 2006). Comparison of FDOM and NO_3 anomalies (Table 3) indicates that dissolved humic substances are produced during the microbial degradation of biogenic organic matter at an average rate of 0.18 ± 0.01, 0.13 ± 0.02 and 0.11 ± 0.05 ppb QS $(\mu M\,N)^{-1}$ at the upper, middle and lower ENACW layers. $\Delta FDOM/\Delta O_2$ ratios ranged from −0.026 in the $<26.95\,kg/m^3$ layer to −0.012 ppb QS $(\mu M\,O_2)^{-1}$ in the $>27.10\,kg/m^3$ layer. These values are in the range of those found on the NW Iberian shelf, 0.14 ± 0.01 ppb QS $(\mu M\,N)^{-1}$ and -0.026 ± 0.003 ppb QS $(\mu M\,O_2)^{-1}$ (Nieto-Cid et al., 2005) and in the Ría de Vigo, -0.029 ± 0.003 ppb QS $(\mu M\,O_2)^{-1}$ (Nieto-Cid et al., 2006). Likewise, these values are similar to those reported by Hayase et al. (1987) in Tokyo Bay (0.09 ppb QS $(\mu M\,N)^{-1}$). It is interesting to note that the $\Delta FDOM/\Delta O_2$ rate calculated for the ENACW upper layer is the same as the rate of production of humic substances by bacterial respiration (0.027 ± 0.003 ppb QS $(\mu M\,O_2)^{-1}$) obtained by Nieto-Cid et al. (2006) after 24 h dark incubations.

5. Conclusions

The frequent spatio-temporal sample collection during the DYBAGA project allowed us to resolve the variability of local aging of ENACW on a year-

round. The analysis of the anomalies of nutrients, fluorescence, oxygen and C_{TC} indicates that there is a seasonal aging with increasing (decreasing) nutrients, fluorescence, and C_{TC} (oxygen) during the summer upwelling, reaching maximum (minimum) values during autumn, associated with the remineralization of biogenic material exported from the euphotic zone after the productive upwelling period. Afterwards, the situation changes dramatically, and we have obtained minimum (maximum) anomalies of nutrients, fluorescence and C_{TC} (oxygen) due to the winter mixing of the water column. Even the distribution of DON anomalies, which responded to short term events during the previous months, presented a clear signal for this period. Thus we can consider that there is a biogeochemical reset of the system during the winter mixing.

For our time series, DOM concentration anomalies were homogenously distributed in the domain of ENACW. Taking into account that we have not observed any correlation between DOM anomalies and inorganic variable anomalies, except for ΔDON vs. ΔNO_3 at ENACW $<26.95\,kg/m^3$, and that there is a significant correlation between ΔDON vs. ΔDOC for the three layers, we suggest that this pattern responds to the solubilisation of fast sinking particles where the rate of solubilisation is larger than the rate of remineralization. For the shallower ENACW layer ($\sigma<26.95\,kg/m^3$), DON is preferential remineralized over DOC, accounting for ~17% of organic matter oxidation at this level.

From the stoichiometry ratios derived from the nutrient, oxygen and C_T concentrations, we have observed fractionation of organic matter remineralization between the upper and lower layers of ENACW. In the mesopelagic layer occupied by ENACW, there is a preferential remineralization of nitrogen- and phosphorus-rich organic matter. In the upper layers of ENACW ($\sigma<27.10\,kg/m^3$), the oxidised organic matter has a percentage >80% in N and P compounds and <20% in carbohydrates and lipids. However, for the deeper ENACW, the percentage of carbohydrates and lipids was ~37% of the oxidised organic matter.

FDOM and nitrate anomalies correlate significantly and directly for the whole ENACW, pointing to the production of dissolved humic substances as a by-product of the microbial degradation of biogenic organic matter. The average rate of this process is 0.18 ± 0.01 ppb QS $(\mu M\,N)^{-1}$ in the upper ENACW layer ($\sigma<26.95\,kg/m^3$), decreasing to 0.11 ± 0.05 ppb QS $(\mu M\,N)^{-1}$ in the lower ENACW layer ($\sigma>27.10\,kg/m^3$).

Acknowledgements

The authors would like to thank the crew of R/V *Mytilus*, the members of the Department of Oceanography of the Instituto de Investigacións Mariñas of Vigo (CSIC) and the Group of Physical Oceanography of the University of Vigo for their valuable help. Financial support for this work came from CICYT project MAR99-1039-C02-01. C.G.C. developed this work with a contract of the Ramón y Cajal programme of the Spanish MCYT. M.N.-C. was funded by a fellowship from the Spanish MCYT.

References

Abell, J., Emerson, S., Renaud, P., 2000. Distributions of TOP, TON and TOC in the North Pacific subtropical gyre: implications for nutrient supply in the surface ocean and remineralisation in the upper thermocline. Journal of Marine Research 58, 203–222.

Álvarez-Salgado, X.A., Miller, A.E.J., 1998. Simultaneous determination of dissolved organic carbon and total dissolved nitrogen in seawater by high temperature catalytic oxidation: conditions for precise shipboard measurements. Marine Chemistry 62 (3, 4), 325–333.

Álvarez-Salgado, X.A., Rosón, G., Pérez, F.F., Pazos, Y., 1993. Hydrographic variability off the Rías Baixas (NW Spain) during the upwelling season. Journal of Geophysical Research 98 (C8), 14447–14455.

Álvarez-Salgado, X.A., Castro, C.G., Pérez, F.F., Fraga, F., 1997. Nutrient mineralization patterns in shelf waters of the Western Iberian upwelling. Continental Shelf Research 17 (10), 1247–1270.

Álvarez-Salgado, X.A., Figueiras, F.G., Pérez, F.F., Groom, S., Nogueira, E., Borges, A.V., Chou, L., Castro, C.G., Moncoiffé, G., Ríos, A.F., 2003. The Portugal coastal counter current off NW Spain: new insights on its biogeochemical variability. Progress in Oceanography 56 (2), 281–321.

Álvarez-Salgado, X.A., Nieto-Cid, M., Gago, J., Brea, S., Castro, C.G., Doval, M.D., Pérez, F.F., 2006. Stoichiometry of the mineralization of dissolved and particulate biogenic organic matter in the NW Iberian upwelling. Journal of Geophysical Research 111, C07017.

Anderson, L.A., 1995. On the hydrogen and oxygen content of marine phytoplankton. Deep-Sea Research I 42, 1675–1680.

Arístegui, J., Agustí, S., Duarte, C.M., 2003. Respiration in the dark ocean. Geophysical Research Letters 30, 1041.

Azam, F., Long, R.A., 2001. Sea snow microcosms. Nature 414, 495–498.

Benner, R., 2000. Missing pieces of the ocean carbon cycle puzzle. OCTEC, Workshop Report (March 7–10). www.msrc.sunysb.edu/octet.

Berger, W.H., Herguera, J.C., 1992. Reading the sedimentary record of the ocean's productivity. In: Falkowski, P.G.,

Woodhead, A.D. (Eds.), Primary Productivity and Biogeochemical Cycles in the Sea. Plenum Press, New York.

Brea, S., Álvarez-Salgado, X.A., Álvarez, M., Pérez, F.F., Mémery, L., Mercier, H., Messias, M.J., 2004. Nutrient mineralization rates and ratios in the eastern South Atlantic. Journal of Geophysical Research 109 (C5), C05030.

Brewer, P.G., Glover, D.M., Goyet, C., Shafer, D.K., 1995. The pH of the North Atlantic Ocean: improvements to the global model for sound absorption in seawater. Journal of Geophysical Research 100 (C5), 8761–8776.

Broecker, W.S., Peng, T.H., 1982. Tracers in the Sea. Lamont-Doherty Geological Observatory. Palisades, New York, 690 pp.

Brzezinski, M.A., 1985. The Si:C:N ratio of marine diatoms: interspecific variability and the effect of some environmental variables. Journal of Phycology 21 (3), 347–357.

Castro, C.G., 1997. Caracterización química del agua subsuperficial del Atlántico Nororiental y su modificación por procesos biogeoquímicos. Ph.D. Thesis, University of Santiago, Spain, 244pp.

Castro, C.G., Álvarez-Salgado, X.A., Figueiras, F.G., Pérez, F.F., Fraga, F., 1997. Transient hydrographic and chemical conditions affecting microplankton populations in the coastal transition zone of the Iberian upwelling system (NW Spain) in September 1986. Journal of Marine Research 55, 321–352.

Castro, C.G., Pérez, F.F., Holley, S.E., Ríos, A.F., 1998. Chemical characterisation and modelling of water masses in the Northeast Atlantic. Progress in Oceanography 41, 249–279.

Chen, R.F., Bada, J.L., 1992. The fluorescence of dissolved organic matter in seawater. Marine Chemistry 37, 191–221.

Clayton, T.D., Byrne, R.H., 1993. Spectrophotometric seawater pH measurements: total hydrogen ion concentration scale calibration of m-cresol purple and at-sea results. Deep-Sea Research II 40 (10), 2115–2129.

del Giorgio, P.A., Duarte, C.M., 2002. Respiration in the open ocean. Nature 420, 379–384.

Emerson, S., Hayward, T.L., 1995. Chemical tracers of biological processes in shallow waters of North Pacific: preformed nitrate distributions. Journal of Marine Research 53, 499–513.

Fiúza, A.F.G., 1984. Hidrologia e dinâmica das águas costeiras de Portugal. Ph.D. Thesis, University of Lisbon, Portugal, 294pp.

Fraga, F., 2001. Phytoplankton biomass synthesis: application to deviations from Redfield stoichiometry. Scientia Marina 65 (2), 153–169.

Hansell, D., Ducklow, H., Macdonald, A.M., Baringer, M.O., 2004. Metabolic poise in the North Atlantic Ocean diagnosed from organic matter transports. Limnology and Oceanography 49 (4), 1084–1094.

Hansen, H.P., Grasshoff, K., 1983. Automated chemical analysis. In: Grasshoff, K., Ehrhadt, M., Kremling, K. (Eds.), Methods of Seawater Analysis. Verlag Chemie, Wheinheim, pp. 347–395.

Hayase, K., Shinozuka, N., 1995. Vertical distribution of fluorescent organic matter along with AOU and nutrients in the equatorial Central Pacific. Marine Chemistry 48, 283–290.

Hayase, K., Yamamoto, M., Nakazawa, I., Tsubota, H., 1987. Behaviour of natural fluorescence in Sagami Bay and Tokio Bay, Japan—vertical and lateral distributions. Marine Chemistry 20, 265–276.

Honjo, S., Manganini, S.J., 1993. Annual biogenic particle fluxes to the interior of the North Atlantic Ocean studied at 34°N 21°W and 48°N 21°W. Deep-Sea Research II 40 (1/2), 587–607.

Honjo, S., Manganini, S.J., Cole, J.J., 1982. Sedimentation of biogenic matter in the deep ocean. Deep-Sea Research 29 (5A), 609–625.

Hopkinson Jr., C.S., Vallino, J.J., 2005. Efficient export of carbon to the deep ocean through dissolved organic matter. Nature 433, 142–145.

Hopkinson Jr., C.S., Fry, B., Nolin, A.M., 1997. Stoichiometry of dissolved organic matter dynamics on the continental shelf of the Northeastern USA. Continental Shelf Research 17 (5), 473–489.

Hung, J.J., Chen, C.H., Gong, G.C., Sheu, D.D., Shiah, F.K., 2003. Distributions, stoichiometric patterns and cross-shelf exports of dissolved organic matter in the East China Sea. Deep-Sea Research I 50 (2), 1127–1145.

Jenkins, W.J., Goldman, J.C., 1985. Seasonal oxygen cycling and primary production in the Sargasso Sea. Journal of Marine Research 43, 465–491.

Karl, D.M., Laws, E.A., Morris, P., Williams, P.J.leB., Emerson, S., 2003. Metabolic balance of the open sea. Nature 426, 32.

Li, Y.H., Peng, T.H., 2002. Latitudinal change of remineralization ratios in the oceans and its implication for nutrient cycles. Global Biogeochemical Cycles 16 (4), 77–71/77–16.

Loh, A.N., Bauer, J.E., 2000. Distribution, partitioning and fluxes of dissolved and particulate organic C, N and P in the eastern North Pacific and Southern Oceans. Deep-Sea Research II 47, 2287–2316.

Lueker, T.J., Dickson, A.G., Keeling, C.D., 2000. Ocean pCO2 calculated from dissolved inorganic carbon, alkalinity, and equations for K1 and K2: validation based on laboratory measurements of CO2 in gas and seawater at equilibrium. Marine Chemistry 70, 105–119.

Martin, J.H., Fitzwater, S.E., Gordon, R.M., Hunter, C.N., Tanner, S.J., 1993. Iron, primary production and carbon-nitrogen flux studies during the JGOFS North Atlantic bloom experiment. Deep-Sea Research I 40 (1/2), 115–134.

McCartney, M.S., Talley, L.D., 1982. The subpolar mode water of the North Atlantic Ocean. Journal of Physical Oceanography 12, 1169–1188.

Milliman, J.D., Troy, P.J., Balch, W.M., Adams, A.K., Li, Y.-H., Mackenzie, F.T., 1999. Biologically mediated dissolution of calcium carbonate above the chemical lysocline? Deep Sea Research I 46 (10), 1653–1669.

Minster, J.F., Boulahdid, M., 1987. Redfield ratios along isopycnal surfaces—a complementary study. Deep-Sea Research 34 (12), 1981–2003.

Mouriño, C., Fraga, F., 1985. Determinación de nitratos en agua de mar. Investigación Pesquera 49, 81–96.

Newton, P.P., Lampitt, R.S., Jickells, T.D., King, P., Boutle, C., 1994. Temporal and spatial variability of biogenic particle fluxes during the JGOFS northeast Atlantic process studies at 47°N, 20°W. Deep-Sea Research 41 (11/12), 1617–1642.

Nieto-Cid, M., Álvarez-Salgado, X.A., Brea, S., Pérez, F.F., 2004. Cycling of dissolved and particulate carbohydrates in a coastal upwelling system (NW Iberian Peninsula). Marine Ecology Progress Series 283, 39–54.

Nieto-Cid, M., Álvarez-Salgado, X.A., Gago, J., Pérez, F.F., 2005. DOM fluorescence, a tracer for biogeochemical

processes in a coastal upwelling system (NW Iberian Peninsula). Marine Ecology Progress Series 297, 33–50.

Nieto-Cid, M., Álvarez-Salgado, X.A., Pérez, F.F., 2006. Microbial and photochemical reactivity of fluorescent dissolved organic matter in a coastal upwelling system. Limnology and Oceanography 51 (3), 1391–1400.

Obernosterer, I., Herndl, G.J., 2000. Differences in the optical and biological reactivity of humic and nonhumic dissolved organic carbon components in two contrasting coastal marine environments. Limnology and Oceanography 45 (5), 1120–1129.

Pérez, F.F., Fraga, F., 1987. A precise and rapid analytical procedure for alkalinity determination. Marine Chemistry 21, 169–182.

Pérez, F.F., Mouriño, C., Fraga, F., Ríos, A.F., 1993. Displacement of water masses and remineralization rates off the Iberian Peninsula by nutrient anomalies. Journal of Marine Research 51, 869–892.

Pérez, F.F., Álvarez, M., Ríos, A.F., 2002. Improvements on the back-calculation technique for estimating anthropogenic CO2. Deep-Sea Research I 49, 859–875.

Pérez, F.F., Castro, C.G., Ríos, A.F., Fraga, F., 2005. Chemical properties of the deep winter mixed layer in the Northeast Atlantic (40–47°N). Journal of Marine Systems 54 (1–4), 115–125.

Sarmiento, J.L., Thiele, G., Key, R.M., Moore, W.S., 1990. Oxygen and Nitrate new production and remineralization in the North Atlantic subtropical gyre. Journal of Geophysical Research 95 (C10), 18303–18315.

Shaffer, G., Bendtsen, J., Ulloa, O., 1999. Fractionation during remineralization of organic matter in the ocean. Deep-Sea Research I 46 (2), 185–204.

Smith, S.V., Hollibaugh, J.T., 1993. Coastal metabolism and the oceanic organic carbon balance. Reviews of Geophysics 31 (1), 75–89.

Sokal, F.F., Rohlf, F.J., 1995. Biometry: The Principles and Practice of Statistics in Biological Research. Freeman and Co, New York, p. 887.

Takahashi, T., Broecker, W.S., Brainbridge, A.E., 1981. The alkalinity and total carbon dioxide concentration in the world ocean. In: Bolin, B. (Ed.), Carbon Cycle Modelling, SCOPE col. 16. Wiley, New York, pp. 271–286.

Takahashi, T., Broecker, W.S., Langer, S., 1985. Redfield ratio based on chemical data from isopycnal surfaces. Journal of Geophysical Research 90 (C4), 6907–6924.

Thomas, C.J., Blair, N.E., Alperin, M.J., DeMaster, D.J., Jahnke, R.A., Martens, C.S., Mayer, L., 2002. Organic carbon deposition on the North Carolina continental shelf slope off Cape Hatteras (USA). Deep-Sea Research II 49 (20), 4687–4709.

Treguer, P., Nelson, D.M., Bennekom, A.J., DeMaster, A., Leynaert, A., Queguiner, B., 1995. The silica balance in the world ocean: a reestimate. Science 268, 375–379.

Unesco, 1985. The International system of units (SI) in oceanography. UNESCO Technical Papers in Marine Science 45, 124.

Wedborg, M., Hoppema, M., Skoog, A., 1998. On the relation between organic and inorganic carbon in the Weddell sea. Journal of Marine Systems 17, 59–76.